Design of a Uniplanar Resonance Phase-Matched Josephson Travelling-Wave Parametric Amplifier

Boon-Kok Tan*† and Ghassan Yassin*
*Department of Physics (Astrophysics), University of Oxford, Keble Road, Oxford OX1 3RH, UK
†Contact: boonkok.tan@physics.ox.ac.uk, phone +44 1865 273 303

***Abstract*—In this paper, we present the design of a resonance phase-matched Josephson travelling-wave parametric amplifier that have a 12 GHz 3 dB-bandwidth centred near 10 GHz. Our design utilises a unilateral planar circuit structure which requires only a single layer of thin superconductor film deposited on a supporting substrate to reduce the fabrication complexity. The nonlinear medium of the device is provided by a series of Josephson junctions embedded in a coplanar waveguide with integrated shunt capacitor, and the dispersion of the transmission line is controlled by quarter wavelength resonators coupled capacitively to the feedline. Here, we describe in detail the electromagnetic designs of the various components of the amplifier, and the coupled-mode equations model that governs the three-wave mixing process. We extract the required circuit parameters of the amplifier through electromagnetic modelling, and determine the parametric gain-bandwidth product of the amplifier using an analytical model. Finally, we discuss the various design aspects that affect the overall performance of the amplifier.**

I. Introduction

For decades, amplification of weak microwave signals with high sensitivity has almost exclusively been achieved using high electron mobility transistors (HEMT) based amplifiers. They are an integral part of many highly sensitive instruments. However, even the best cryogenic low noise amplifiers (LNAs) to date can only reach noise temperatures of $T_N \approx 2\,\mathrm{K}$ at 4–8 GHz; well above the quantum limit of $h\nu/kB \approx 48$ mK/GHz value. Furthermore, these LNAs are power hungry with substantial heat dissipation which can present a serious limitation in many applications, in particular in large format arrays. In recent years, travelling wave parametric amplifiers (TWPAs) have been drawing increasing attentions due to their potential to achieve quantum-limited noise performance at a large bandwidth. These amplifiers can be scaled easily to operate from radio to THz frequencies and they are easy to fabricate and integrate with other detector circuits, which is useful for many applications such as readout for astronomical detectors [1], [2] and superconducting qubits experiments [3].

The principle of operation of a parametric amplifier relies on the nonlinear impedance of a transmission medium to mediate energy exchange between signals of different frequencies through a wave-mixing process. Amplification can be achieved through varying one of the medium's nonlinear parameters (e.g., reactance) by applying a strong 'pump' signal at a frequency f_P. If a weak signal at frequency f_S is also applied to the medium, under specific conditions, the time-varying reactance may transfer power from the pump to the signal, thereby achieving amplification. During the mixing process, a third frequency component, the 'idler' at $f_I = 2f_P - f_S$ is also generated and amplified as well. Because the amplification mechanism relies purely on the nonlinear reactance, the dissipation can be made arbitrarily small and Johnson noise can be eliminated, allowing the quantum limit to be reached.

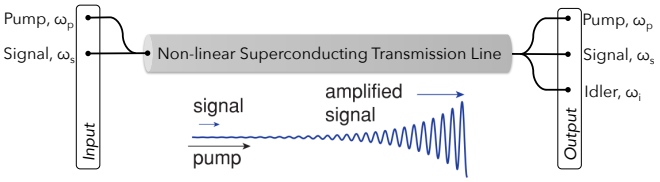

(a) Travelling Wave Parametric Amplifier

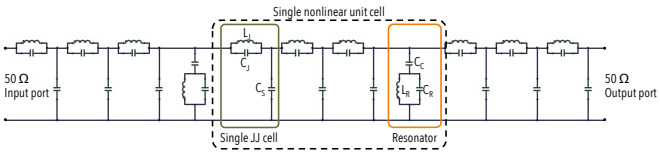

(b) Circuit Model

Fig. 1. (a) A schematic diagram illustrating the three-wave mixing process in a long nonlinear medium that mediates the energy transfer from the pump wave to the signal wave for amplification. (b) Part of the circuit model used to describe the JTWPA, showing the individual nonlinear unit cell comprising three JJ units and a resonator. Each JJ is shunted with a capacitor to engineer the characteristic impedance of the transmission line.

The nonlinear behaviour of the transmission line reactance can be realised either via the intrinsic kinetic inductance of a superconducting material [4], [5], [6], [7], [8] or through the inductance of Josephson junctions [9], including the use of superconducting quantum interference devices (SQUIDs) [10]. To reach high gain, the signal must interact strongly with the nonlinear medium. This has traditionally been realised by enclosing the nonlinear medium in a resonant cavity, resulting in an intrinsically narrow band performance. As shown in Fig. 1, this limitation can be lifted by operating the device in the travelling wave regime with long propagation length. This approach has a much more promising potential for achieving the broad bandwidth required in many applications.

In what follows, we shall focus on the design of a Josephson junction based TWPA (JTWPA) developed specifically as a readout amplifier for a qubit experiment which requires quantum-limited noise figure for its highly sensitive operation. A TWPA employing a series of Josephson junctions (JJs) embedded in a long transmission line has already been successfully demonstrated [9], [11]. However, most of the existing designs require multiple-layer fabrication, which needs complex processing procedures. In our JTWPA design, we therefore use only a single layer circuit components to construct the amplifier chip, simplifying the fabrication process and improving the fabrication yield. This simplicity in fabrication is achieved on the expense of challenges in the design of the JTWPA,

978-1-5386-2720-4/17/$31.00 ©2017 IEEE

but as will be shown later, with careful consideration we can achieve high-performance design without compromising the transmission losses, bandwidth and other figures-of-merit of the JTWPA.

II. JTWPA Design

There are four critical aspects to the design of a TWPA: 1) the use of nonlinear transmission line as the gain medium; 2) suppression of higher harmonics generation from the pump to prevent formation of the shock waves; 3) design of low-loss transmission lines to carry the signal; and 4) the creation of phase-matching structures along the transmission to achieve high exponential gain over a broad bandwidth. The use of JJs embedded in a transmission line allows us to achieve the first two aspects simultaneously, as the junction's plasma resonance frequency naturally prohibits the propagation of higher harmonics in the transmission line and hence prevents the formation of shock waves.

To achieve low loss, we employ a 200 nm thick superconducting aluminium coplanar waveguide (CPW) deposited on a 500 μm thick silicon substrate as the transmission medium. Compared to other uniplanar transmission lines such as coplanar striplines (CPS) or slotlines, CPW is an unbalanced transmission line, hence the junctions can easily be embedded in the signal carrying central strip instead of both electrodes. The thickness of the thin film was chosen to make the surface resistance loss negligible, without the complexity of depositing much thicker film, as shown in Fig. 2. The central strip width of the CPW is set to be 10 μm, with 5.5 μm wide gaps between the central strip and the ground plane to realise a Z_0 =50 Ω characteristic impedance line. The Josephson junctions used here have a junction capacitance of $C_J = 48$ fF and a junction inductance of $L_J = 100$ pH.

The inclusion of the Josephson junctions in the CPW line will clearly alters the initial characteristic impedance value. We therefore need to capacitively shunt the junction to match the JJs-loaded CPW line to the 50 Ω input and output interfaces. To avoid using parallel plate capacitors and other complicated uniplanar structures such as interdigit capacitor, we achieve this by introducing a simple alteration to the CPW line. Fig. 3(a) shows how a uniplanar shunt capacitor is incorporated into the JJs-line. The CPW section after each junction is connected to a fish-bone-like structure comprising a group of 4-fingers , with each finger having the same width and gap dimension as the 50 Ω CPW. The finger length is about 50 μm long, and each fish-bone cell is placed at 20 μm after the JJ. These dimensions were optimised using the full 3D electromagnetic (EM) simulator, Ansys High Frequency Structure Simulator (HFSS), including the effect of superconductivity. As shown in Fig. 3(b), with this alteration, we managed to reduce the return loss of a 30-JJs long CPW line (connected to 50 Ω input/output port) from –10 dB to less than –30 dB.

The final criteria listed above can be achieved by incorporating phase-shifter circuits in the transmission line. The phase-shifters provide a mean to engineer the required phase relation between the pump, the signal and the idler wave for maximum gain. This dispersion engineering is usually realised

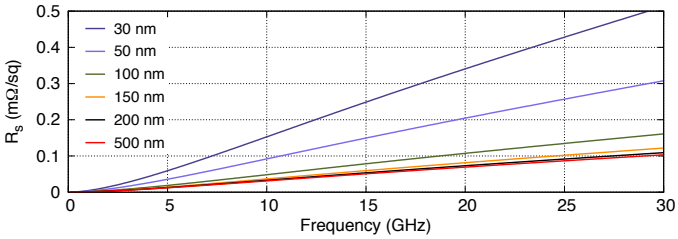

Fig. 2. A plot showing the surface resistance (R_s) of a superconducting aluminium thin film as a function of frequency for various thickness, calculated from the Mattis-Bardeen equation.

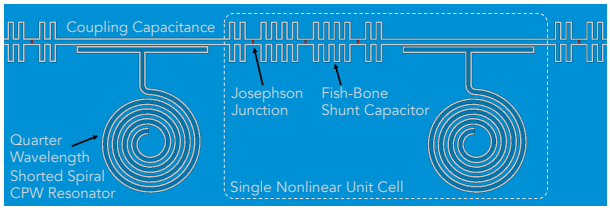

(a) Single nonlinear unit cell

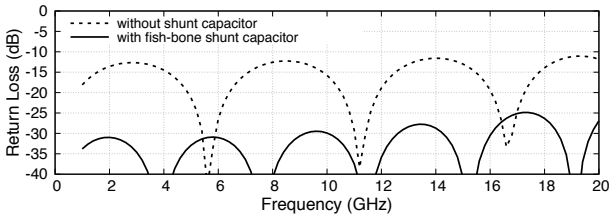

(b) HFSS simulated return losses of a 30-JJs long CPW line

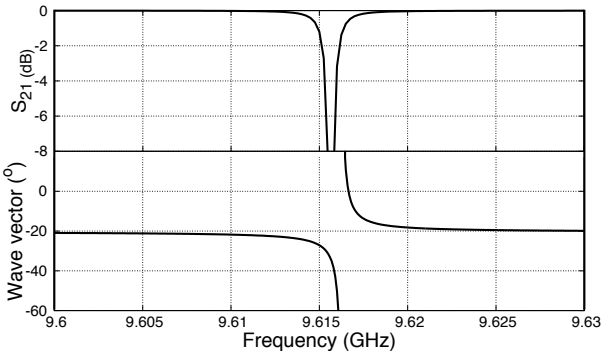

(c) Stopband and wave vector divergence created by the resonator

Fig. 3. Circuit implementation of the JJs embedded CPW line with shunt capacitors for impedance transformation, coupled with spiral resonators; and the simulated responses of the individual components.

by using either periodic structures or resonators, to create a stopband in the otherwise approximately linear dispersion transmission line. The periodic structure option, which require a large number of elements spaced at large distance (typically $\lambda/2$) to achieve the required phase shift, is not suitable for JJs embedded line that have very high nonlinear inductance per guided wavelength. In our design, we have chosen a simpler quarter wavelength resonator architecture, as shown in Fig. 3(a). The long $\lambda/4$ CPW line is folded into a spiral form to both obtain a large enough geometric inductance and maintain a compact design. The spiral resonator is terminated with a short, and electromagnetically coupled to the main feedline via another CPW placed adjacent to the feedline. All these CPW components have the same dimension as the main feedline. The design of the spiral resonator and the coupler was also

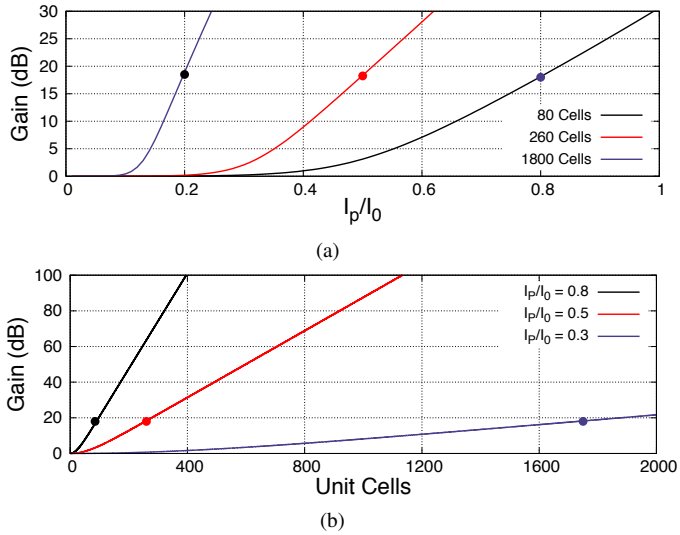

Fig. 4. The relation between the peak gain of the amplifier at 10 GHz with (a) the pump current and (b) the length of the transmission line.

obtained via 3D HFSS modelling to ensure that it resonates at the desired frequency with the the required Q-factor. The result is shown in Fig. 3(c), where the stopband frequency is clearly seen near 9.616 GHz, with closed to 0 dB insertion loss away from the resonance frequency. The resonance frequency was chosen to achieve peak gain at 10 GHz.

III. Analytical Model & Analysis

The method of analysis we have used models the JTWPA as a passive device. To perform wave-mixing and to predict the parametric gain of the JTWPA, we use a coupled-mode equation model. This method has been described in detail in previous publications, hence we only summarise the treatment outlined by [12] here, with one exception. In our implementation, the circuit components comprising the transmission line were described through $ABCD$ scattering matrices of a 2-port network to allow for the flexibility of applying the same equations to different circuits without the need to re-derive the equations from first principle. The circuit parameters describing the JTWPA required for this theoretical model were extracted from the EM models described above.

Using a first principles model for the nonlinear dynamics in the JJs embedded transmission line, and by making the ansatz that the solutions are travelling waves, together with the slowly varying envelope approximation, and neglecting pump depletion, a set of coupled wave equations for the signal and idler waves can be obtained as:

$$\begin{aligned} \frac{\partial a_s}{\partial x} - i\kappa_s a_i^* e^{i(\Delta k_L + 2\alpha_p - \alpha_s - \alpha_i)x} &= 0 \\ \frac{\partial a_i}{\partial x} - i\kappa_i a_s^* e^{i(\Delta k_L + 2\alpha_p - \alpha_s - \alpha_i)x} &= 0 \end{aligned} \tag{1}$$

where a_s and a_i and are the amplitudes of the signal and idler respectively; κ_s, and κ_i are the corresponding coupling factors that depend on the circuit parameters and scale quadratically with the pump current; and α_p, α_s, α_i represent the phase change of the pump, signal and the idler respectively as a result of modulation by the pump wave. The phase mismatch of the three signals as a result of linear propagation is given by $\Delta k_L = 2k_p - k_s - k_i$.

The above simplifications of the coupled equations allow the the amplitudes of the propagating waves to be calculated analytically with a solution that can be written in the form of

$$a_s(x) = a_{s,0}\left[\cosh(gx) - \frac{i\Delta k}{2g}\sinh(gx)\right] e^{i\Delta k x/2} \tag{2a}$$

$$a_i(x) = \frac{\kappa_1}{g} a_{s,0}^* \sinh(gx) e^{i\Delta k x/2}, \tag{2b}$$

where g is the gain factor and $\Delta k = \Delta k_L + 2\alpha_p - \alpha_s - \alpha_i = 0$ is the total phase mismatch. Assuming no idler at the input field, the gain coefficient is given by:

$$g = \sqrt{\kappa_s \kappa_i^* - \frac{\Delta k^2}{4}}. \tag{3}$$

The last equation implies that maximum parametric gain g can be achieved when the phase mismatch $\Delta k = 0$. Therefore, by locating the pump wave near the resonance where the dispersion diverge exponentially away from the linear relation (see Fig. 3(c)), the amount of dispersion Δk may be adjusted to optimise the gain.

Using this analytical model along with the circuit parameters derived from the EM models, we can now predict the gain-bandwidth product of our JTWPA. Our aim is to design a JTWPA that have a gain coefficient higher than 15 dB in the frequency range from 4–16 GHz (120%). The gain of a TWPA can be controlled easily, either via the amplitude of the pump current I_P or the total length L of the nonlinear transmission medium. This is shown graphically in Fig. 4, which clearly demonstrates that the effect of one parameter on the gain is inversely proportional to the effect of the other. In other words, a given gain value achieved by driving the JTWPA with high pump current requires a short transmission line, since the device is now operating in higher nonlinearity region and the gain medium is being utilised more efficiently.

In Fig. 5, we show how the same gain-bandwidth products can be achieved with different combination of I_P and L i.e., 1) I_P/I_0 = 0.8 which requires 80 nonlinear unit cells; 2) I_P/I_0 = 0.5 with 260 nonlinear unit cells; and 3) I_P/I_0 = 0.2 with 1800 nonlinear unit cells. One notes that the required length to achieve the same peak gain for lower I_P is much longer than the opposite case. Reducing the pump current by a factor of four requires almost 22.5× longer transmission line. We will now show that a longer transmission line with a large number of JJs and resonators has major disadvantages.

Clearly, a longer transmission line is prone to fabrication errors and lower the yield, but more importantly, it can have severe effect on the gain stability if the input/output interfaces of the amplifier are not properly matched. We have investigated this effect by using the same set of circuit parameters to form a full circuit model in Ansys Electronic Desktop Circuit Design package, and increasing the input/output port impedance of the circuit model from 50 Ω to 75 Ω. As clearly shown in Fig. 6, this causes the insertion loss of the amplifier to vary sinusoidally due to standing waves. This means that the pump current injected into the amplifier will now oscillate at a certain frequency that depends on the length of the transmission line.

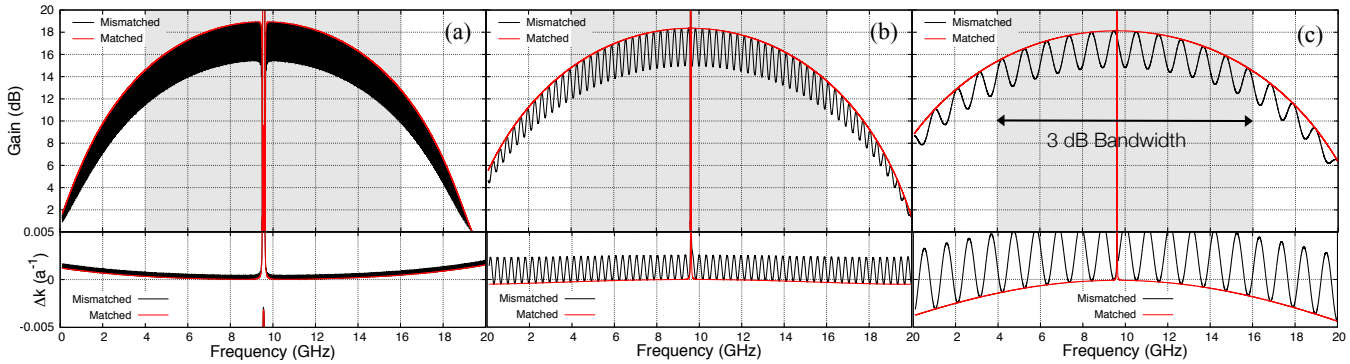

Fig. 5. Gain profile and dispersion relation of the JTWPA at three different operational modes. The plots were made with L_J =100 pH, C_J=48 fF, shunt capacitance C_S=37 fF, coupling capacitance C_c=2 fF, resonator capacitance C_R=212.95 fF, and resonator inductance L_R=1.274 nH. (a) I_P/I_0=0.2, L = 1800 unit cells, f_P=9.5633 GHz (b) I_P/I_0=0.5, L = 260 unit cells, f_P=9.60763 GHz (c) I_P/I_0=0.5, L = 80 unit cells, f_P=9.61275 GHz.

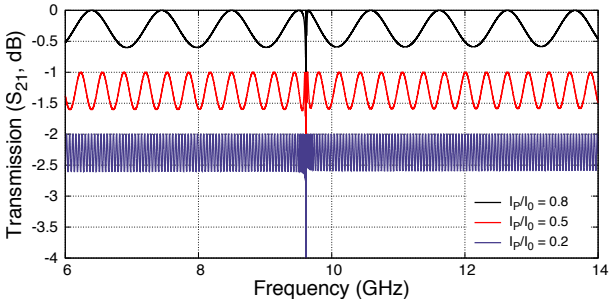

Fig. 6. Profile of insertion loss with impedance mismatch at the input/output port of the circuit model showing the transmission fluctuation caused by the standing wave. The red and blue curves were offset by 1 dB and 2 dB correspondingly for clarity.

As seen in Fig. 4(a), a small changes in I_P could result in large deviation in gain, causing the gain to oscillate as observed in many experiments reported in the literature. This effect is illustrated in Fig. 5, where the amplitude of the pump current in the coupled-mode equation model was multiplied by a frequency dependence coefficient to emulate the sinusoidal fluctuation of the insertion loss shown in Fig. 6. The gain can now be seen to oscillate at about 3 dB level, compared to the smooth gain profile without the ports mismatch, even though the insertion loss was only varied by about –0.5 dB level.

The frequency of the gain oscillation is directly proportional to the length of the transmission line, which suggests that the gain profile of the amplifier would be extremely noisy if the transmission line is too long, such as those shown in Fig. 5(a) & (b). Hence, we argue that to increase the gain, it is more advantageous to operate the amplifier at higher pump level to ensure that the required nonlinear medium is as short as possible. Although this technique does not completely get rid of the ripple effect, we expect it to give much smoother gain profile with proper impedance matching at the input/output interface, as those shown in red in Fig. 5. Furthermore, if the gain has a low oscillation frequency, this effect could potentially be calibrated out or compensated for by incorporating a programmable microwave attenuator to control the amplitude of the pump current to flatten the gain curve. This is particularly useful for applications that need to amplify high-Q signals, such as readouts for the Kinetic Inductance Detectors (KIDs), where lower periodicity would make it easier to identify the signal of interest.

IV. Conclusion

We have presented a uniplanar JTWPA design using rigorous electromagnetic modelling. By deriving the circuit parameters from the EM models and exporting them to the coupled mode equations, we investigated the operational conditions and the resulting parametric gain-bandwidth product of our JTWPA. We have used this model to design a TWPA with 15 dB gain from 4–16 GHz, where the gain peak at about 18 dB.

References

[1] C. Bockstiegel, J. Gao, M. Vissers, M. Sandberg, S. Chaudhuri, A. Sanders, L. Vale, K. Irwin, and D. Pappas, "Development of a broadband nbtin traveling wave parametric amplifier for mkid readout," *Journal of Low Temperature Physics*, vol. 176, no. 3-4, pp. 476–482, 2014.

[2] K. D. Irwin and K. W. Lehnert, "Microwave squid multiplexer," *Applied physics letters*, vol. 85, no. 11, pp. 2107–2109, 2004.

[3] M. H. Devoret and R. J. Schoelkopf, "Superconducting circuits for quantum information: an outlook," *Science*, vol. 339, no. 6124, pp. 1169–1174, 2013.

[4] B. H. Eom, P. K. Day, H. G. Leduc, and J. Zmuidzinas, "A wideband, low-noise superconducting amplifier with high dynamic range," *Nature Physics*, vol. 8, no. 8, p. 623, 2012.

[5] S. Chaudhuri, D. Li, K. Irwin, C. Bockstiegel, J. Hubmayr, J. Ullom, M. Vissers, and J. Gao, "Broadband parametric amplifiers based on nonlinear kinetic inductance artificial transmission lines," *Applied Physics Letters*, vol. 110, no. 15, p. 152601, 2017.

[6] M. R. Vissers, R. P. Erickson, H.-S. Ku, L. Vale, X. Wu, G. Hilton, and D. P. Pappas, "Low-noise kinetic inductance traveling-wave amplifier using three-wave mixing," *Applied physics letters*, vol. 108, no. 1, p. 012601, 2016.

[7] A. Adamyan, S. de Graaf, S. Kubatkin, and A. Danilov, "Superconducting microwave parametric amplifier based on a quasi-fractal slow propagation line," *Journal of Applied Physics*, vol. 119, no. 8, p. 083901, 2016.

[8] W. Shan, Y. Sekimoto, and T. Noguchi, "Parametric amplification in a superconducting microstrip transmission line," *IEEE Transactions on Applied Superconductivity*, vol. 26, no. 6, pp. 1–9, 2016.

[9] C. Macklin, K. O'Brien, D. Hover, M. Schwartz, V. Bolkhovsky, X. Zhang, W. Oliver, and I. Siddiqi, "A near–quantum-limited josephson traveling-wave parametric amplifier," *Science*, vol. 350, no. 6258, pp. 307–310, 2015.

[10] A. Zorin, M. Khabipov, J. Dietel, and R. Dolata, "Traveling-wave parametric amplifier based on three-wave mixing in a josephson metamaterial," *arXiv preprint arXiv:1705.02859*, 2017.

[11] T. White, J. Mutus, I.-C. Hoi, R. Barends, B. Campbell, Y. Chen, Z. Chen, B. Chiaro, A. Dunsworth, E. Jeffrey, *et al.*, "Traveling wave parametric amplifier with josephson junctions using minimal resonator phase matching," *Applied Physics Letters*, vol. 106, no. 24, p. 242601, 2015.

[12] K. O'Brien, C. Macklin, I. Siddiqi, and X. Zhang, "Resonant phase matching of josephson junction traveling wave parametric amplifiers," *Physical review letters*, vol. 113, no. 15, p. 157001, 2014.